의학 박사 학위 논문

기도 스텐트 개량을 위한 연구: 동물모델의 수립 및 새로 개발한 기도 스텐트 (GINA stent)를 이용한 전임상시험

Research for airway stent improvement: Establishment of animal model and preclinical study using newly developed airway stent (GINA stent)

울 산 대 학 교 대 학 원

의 학 과

김 진 형

기도 스텐트 개량을 위한 연구: 동물모델의 수립 및 새로 개발한 기도 스텐트 (GINA stent)를 이용한 전임상시험

지 도 교 수　이 태 훈

이 논문을 의학박사 학위 논문으로 제출함

2022 년 2 월

울 산 대 학 교　대 학 원

의　학　과

김 진 형

김진형의 의학박사학위 논문을 인준함

심사위원 안 종 준 (인)

심사위원 이 태 훈 (인)

심사위원 제갈양진 (인)

심사위원 나 승 원 (인)

심사위원 엄 중 섭 (인)

울 산 대 학 교 대 학 원

2022 년 2 월

ABSTRACT

Background and purpose: Central airway obstruction (CAO) is broadly defined as a blockage of the trachea, either main stem bronchus, and/or the bronchus intermedius, which can frequently cause dyspnea, asphyxiation, and even death. Surgery could provide the opportunity for definitive management. However, surgical treatment is not indicated for advanced and/or metastatic disease or poor medical conditions. In these situations, bronchoscopic intervention with airway stents is a useful treatment option. Despite the effectiveness of the airway stents for immediate relief of CAO, they occasionally cause critical complications such as migration, mucostasis, and granulation tissue formation. For this reason, researchers are continuously striving to solve these problems with an appropriate animal model. Several animal models of tracheal stenosis have been developed through various methods. However, existing models take a long time to develop (3–8 weeks). In the present study, we attempted to establish a fast tracheal stenosis model in pigs (part I). And with the model, we evaluated the performance of our newly developed silicone airway stents (GINA and custom GINA stents) that intended to overcome the shortcomings of existing stents (part II and III). The GINA stent improved the anti-migration design using right-angled triangle-shaped outer rings for the cartilaginous trachea and a raised, three-line arrangement for the membranous trachea; tried to maintain the airway's physiological role with a flexible and dynamic structure though using a flat part, similar to the membranous portion of the tracheobronchial tree; and added a radiopaque material to check positioning more easily.

Materials and methods: In part I, we sought to establish a new and fast tracheal stenosis model in pigs using a combination of cuff overpressure intubation (COI) and electrocautery. Fourteen pigs were divided into three groups: tracheal cautery (TC) group (n=3), COI group, and COI-TC combination group (n=8). Cuff overpressure (200/400/500 mmHg) was applied using a 9-mm endotracheal tube. Tracheal cautery (40/60 watts) was performed using a rigid bronchoscopic electrocoagulator. After the intervention, the pigs were observed for three weeks and bronchoscopy was performed every seven days. When the cross-sectional area decreased by > 50%, it was confirmed that tracheal stenosis was established. Part II study was the evaluation of mechanical characteristics and performance of the novel GINA stent using the established pig tracheal stenosis model. All the tests involved the comparison of the GINA stent [outer diameter (OD, mm): 14; length (L, mm): 55] with the Dumon stent (OD: 14; L: 50). The mechanical tests were performed using a digital force gauge, in order to determine the anti-migration force,

expansion force, and flexibility. The present study evaluated the short-term (3 weeks) performance of the two stents after implantation [GINA (n = 4) vs. Dumon (n = 3)] in the pig tracheal stenosis model. In part III, we developed a 3D-engineered personalized airway stent (custom GINA stent) hybridizing GINA stent design and evaluated its short-term performance in the pig model of tracheal stenosis. A custom GINA stent was fabricated by computer-aided design using computed tomography scan data of a pig, and the stent was inserted into the pig with induced tracheal stenosis, and evaluated the performance for 3 weeks. The experiment was attempted in two pigs to evaluate the feasibility of the custom GINA stent.

Results: In part I, the time for tracheal stenosis was 14 days in the TC group and 7 days in the COI-TC combination group. In the COI group, no stenosis occurred. In the COI-TC group, electrocautery (40 watts) immediately after intubation for >1 h with a cuff pressure of 200 mmHg or more resulted in sufficient tracheal stenosis within 7 days. Moreover, the degree of tracheal stenosis increased in proportion to the cuff pressure and tracheal intubation time. In part II, the results about the comparison of the mechanical properties of the GINA and Dumon stents are stated as follows: anti-migration force (18.4 vs. 12.8 N, P = 0.008); expansion force (11.9 vs. 14.5 N, P = 0.008); and flexibility (3.1 vs. 4.5 N, P = 0.008). The short-term performance of the GINA and Dumon stents are stated as follows: mucus retention (0/4 vs. 0/3); granulation tissue formation (0/4 vs. 0/3); and migration (1/4 vs. 2/3). In part III, the stent fabrication took 16 days for the first pig, but was reduced to 7 days for the second pig. In both, the stents were in situ over 3 weeks, and neither granulation tissue formation at either end nor mucostasis was observed.

Conclusion: The combined use of cuff overpressure and electrocautery helped to establish tracheal stenosis in pigs rapidly (part 1). The GINA stent displayed better mechanical properties and comparable short-term performance compared to the Dumon stent (part II). Lastly, we developed an individualized airway stent (custom GINA stent) with a novel design using 3D engineering within seven days, and the short-term stent performance showed the plausibility (part III).

Keywords: Silicone airway stent; tracheal stenosis; pig tracheal stenosis model; 3D printing; custom airway stent

CONTENTS

PART III: 3D-engineered personalized airway stent (custom GINA stent): introduction and performance evaluation in pigs

LIST OF TABLES

LIST OF FIGURES

LIST OF ABBREVIATIONS

ARRIVE	Animal research: reporting of in vivo experiments
3D	Three dimensional
CAO	Central airway obstruction
CAD	Computer-aided design
COI	Cuff overpressure intubation
CT	Computed tomography
ID	Internal diameter
L	Length
N	Newton
OD	Outer diameter
RD	Ring diameter
SD	Standard deviation
TC	Tracheal cautery

PART I

Rapid Establishment of Tracheal Stenosis in Pigs Using Endotracheal Tube Cuff Overpressure and Electrocautery

INTRODUCTION

Central airway obstruction (CAO) is broadly defined as obstruction of the trachea, either of the main stem bronchus and/or the bronchus intermedius [1]. It might occur secondary to tumors, tracheal intubation, or infection. CAO can frequently cause dyspnea, asphyxiation, and even death. In cases of benign CAO, surgery is the treatment of choice. However, in cases with contraindication to surgery, bronchoscopic intervention is a potentially useful treatment option. Similarly, in malignant CAO, surgery can be performed if it is operable, but bronchoscopic intervention is performed in cases of inoperable advanced cancer or terminal cancer.

A variety of endoscopic procedures are available to alleviate CAO. Balloon dilation, airway stent, mass excision (debulking), and tumor ablation (laser therapy, cryotherapy, argon plasma coagulation, electrocautery, and photodynamic therapy) have been used [2]. However, the management of CAO remains difficult. To investigate and develop a new effective treatment for CAO, it is necessary to establish an experimental animal model. Several animal (dog, pig, and rabbit) models of tracheal stenosis have been developed through various methods such as chemical caustic agents, laser, and electrocautery [7-10]. Nonetheless, these methods are sophisticated and require a relatively longer time (3–8 weeks) to induce stenosis. Moreover, these models are inconsistent with the actual mechanism of human tracheal stenosis. Prolonged intubation and tracheostomy are the most common causes of human benign tracheal stenosis. The actual mechanisms underlying this stenosis include a combination of (1) excessive cuff pressure, (2) over-sized intubation tube, and (3) tracheal injury. Local ischemia caused by either excessive cuff pressure or an over-sized intubation tube and tracheal injury (trauma during intubation, or tracheostomy related injury) can result in regional inflammation and subsequent stenosis during healing [11-13].

Recently, Su et al reported that prolonged intubation (24 hours) with cuff-overpressure and an oversized tube could induce tracheal stenosis in dogs in a relatively shorter time (2 weeks) [14]. This study inspired our research. We hypothesized that if three mechanisms (excessive cuff pressure, over-sized intubation tube, and tracheal injury) are applied at the same time, it would be possible to establish an animal tracheal stenosis model more quickly.

The purpose of the present study was to establish a new and rapid animal model of tracheal stenosis in pigs through the combined use of prolonged over-sized intubation with cuff-overpressure and tracheal injury (tracheal cautery), and investigate the difference in the incidence and speed of tracheal stenosis development according to the degree of cuff overpressure, intubation duration, and tracheal injury (tracheal cautery).

MATERIALS AND METHODS

Animals

Twelve-week-old female farm pigs (weight, 40–45 kg; tracheal size, 16–20 mm) were used because their tracheal size is similar to that of humans. The animal experiments were conducted at the preclinical trial center of Pusan National University Yangsan Hospital. The experimental animals were handled according to well-established bioethical guidelines (Guiding Principles in the Care and Use of Animals, DHEW Publication, NIH), following a protocol approved by the Institutional Animal Care and Use Committee at Pusan National University Yangsan Hospital (Approval Number: PNUYH-2017-043).

General Anesthesia

Intramuscular alfaxan (5 mg/kg) and inhalational 3% isoflurane were used for the induction and maintenance of general anesthesia, respectively.

Tracheal Cautery

Tracheal cautery (TC) (40–60 watts) was performed using a coagulation suction tube (10390 BN, Karl Storz, Germany) via a rigid bronchoscope (size 8.5, 10318 BP, Karl Storz, Germany)

(Figure 1). The cautery was performed at eight sites (including the membranous portion) of the tracheal segment usually 5 cm below the vocal cords at a length of 1 cm parallel to the trachea. Cautery was performed after (prolonged) cuff overpressure intubation, at the position where the cuff was located.

Figure 1. The equipment used for tracheal cautery

a. Rigid bronchoscope (size 8.5, 10318 BP, Karl Storz, Germany).

b. Coagulation suction tube (10390 BN, Karl Storz, Germany).

c. The cautery was performed on eight sites (including the membranous portion) of the tracheal segment for a length of 1 cm parallel to the trachea.

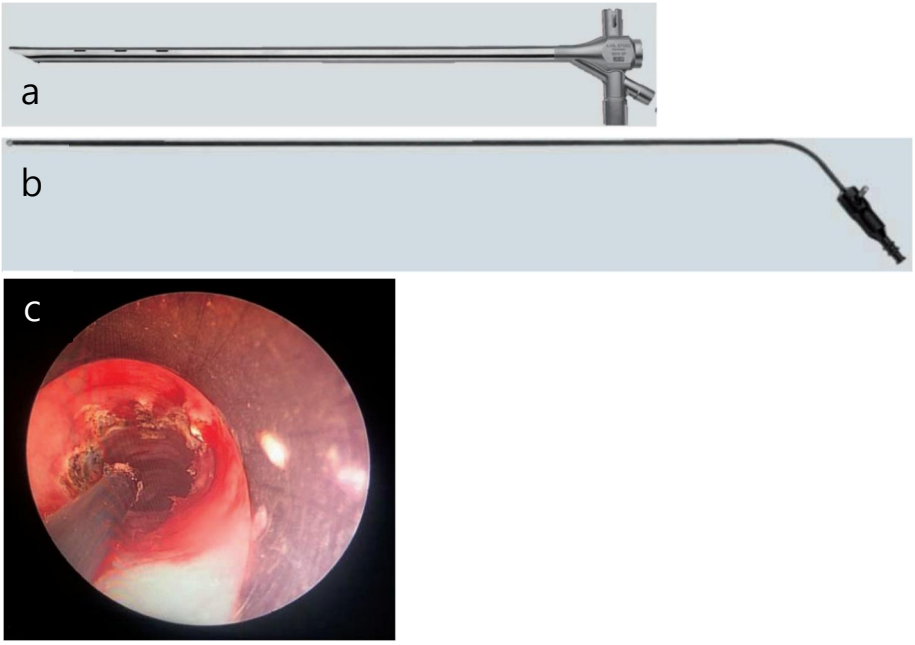

Cuff Overpressure Intubation with An Oversized Tube

A cuffed silicone endotracheal tube with an internal diameter of 9 mm (ID9)/outer diameter of 12 mm (OD12), and length of 33 cm (HS-ET-WC9.0W/ NC9.0W, Hyupsung Medical, Korea) was selected as the over-sized tube, because tubes larger than ID9/ OD12 were technically difficult to intubate. The proximal tip of the tube was placed 5 cm deeper than the upper incisor of the pig to ensure the cuff of the tube was located at least 5 cm below the vocal cords: this is because the 33 cm-long endotracheal tube was a little short for pigs. A homemade pressure measuring device was used to monitor and maintain cuff overpressure (200–500 mmHg) (Figure 2). The tracheal tube used in the present study was unable to withstand cuff pressures higher than 500 mmHg, limiting the maximum load of the cuff to 500 mmHg. Due to the laboratory operating time constraint, the cuff overpressure intubation (COI) period was limited to a maximum of 8 hours.

Figure 2. Homemade cuff-pressure measuring device

a. The device is composed of a three-way connector, aneroid barometer, and air bulb.

b. After the cuff pressure was raised to the target pressure via an air bulb, general anesthesia was maintained. The pressure gauge was checked every 10 min and air was injected into the air bulb if it dropped below the target pressure.

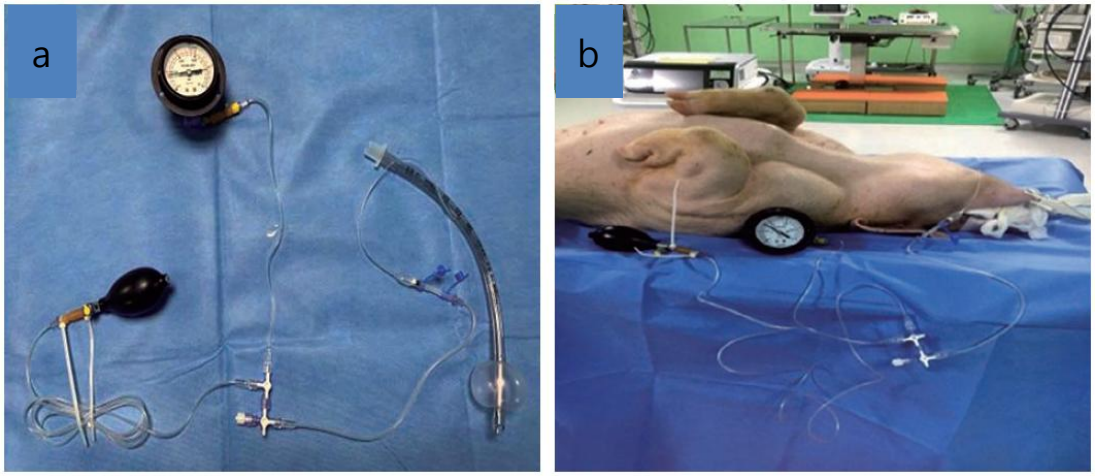

Tracheal Stenosis

The tracheal lumen was examined using a flexible bronchoscope (MAF-TM, Olympus, Japan) on a weekly basis and the tracheal diameter was calculated considering the opening diameter of the biopsy forceps. The degree of tracheal stenosis was determined by the reduction of the tracheal lumen cross-section area: $(S - s)/S \times 100\%$, where "s" is the tracheal cross-sectional area after the intervention and "S" is the area before the intervention. A reduction of at least 50% of the measured airway cross-sectional area after intervention indicated establishment of a successful model. During the observation period, pigs exhibiting dyspnea, pain, costal retraction, or significant tracheal stenosis were euthanized using KCl injection. Pigs without any signs of breathing difficulty or fatal tracheal stenosis were euthanized on day 21. After euthanasia, tracheas were removed for hematoxylin and eosin staining to observe histologic changes.

Study Groups

Experiments were performed on 14 pigs, which were divided into three groups: TC group (n=3), COI group (n=3), and COI-TC combination group (n=8) (Table 1). In the TC group (n=3), one pig (Pig TC1) received 60 watts electrocautery, and the other two pigs (Pig TC2 and TC3) received 40 watts electrocautery. In the COI group (n=3), prolonged intubation with cuff overpressure was applied to the pigs after endotracheal tube (ID9/OD12) insertion. Pigs (Pig COI1, COI2, and COI3) were intubated for 8 h with 200, 400, and 500 mmHg cuff pressure, respectively. In the COI-TC combination group (n=8), immediately after COI (ID9/OD12 tracheal tube) at various cuff pressures (200–500 mmHg) and intubation durations (0.5–8 h), electrocautery (40 watts) was performed on the tracheal mucosa where the cuff was located. In the TC group, if stenosis did not occur, repeated cautery was performed. However, no further intervention was allowed in the other groups.

Table 1. Details of the intubation duration, cuff pressure, tracheal cautery, and results of the tracheal stenosis model

Pig No. (n=14)	Tracheal inner diameter on day 0, mm	Tracheal cross-sectional area, mm^2	Cuff overpressure intubation (COI) with ID 9.0 (OD 12) tube, day 0		Tracheal cautery (TC), watt			Tracheal inner diameter, mm		Tracheal cross-sectional area, mm^2		Stenosis, %		Length of stenosis, mm	Survival period, days
			Cuff pressure, mmHg	Intubation duration, hour	Day 0	Day 7	Day 14	Day 7	Day 14	Day 7	Day 14	Day 7	Day 14		
TC1	16	201	—	—	60	—	—	13	—	133		34	—	15	7
TC2	17	227	—	—	40	40	—	14	10	154	79	32	65	18	21
TC3	18	254	—	—	40	40	—	15	11	177	95	31	63	20	21
COI1	17	227	200	8	—	—	—	16	16	201	201	11	11	15	21
COI2	16	201	400	8	—	—	—	15	15	177	177	12	12	14	21
COI3	16	201	500	8	—	—	—	15	16	177	201	12	0	20	21
COI-TC1	15	177	500	8	40	—	—	5	—	20	—	89	—	25	7
COI-TC2	17	227	500	4	40	—	—	7	6	38	28	83	88	30	14
COI-TC3	18	254	400	4	40	—	—	8	7	50	38	80	85	25	14
COI-TC4	17	227	400	2	40	—	—	9	9	64	64	72	72	25	14
COI-TC5	18	254	400	1	40	—	—	11	10	95	79	63	69	20	21
COI-TC6	16	201	400	0.5	40	—	—	11	10	95	79	53	61	22	21
COI-TC7	17	227	200	1	40	—	—	12	11	113	95	50	58	20	21
COI-TC8	18	254	200	0.5	40	—	—	15	14	177	154	31	40	15	21

RESULTS

The results of the 14 pigs in the three groups are summarized in Table 1. Detailed results of the groups are as follows.

TC Group

In the TC group (n=3), the pig that received 60 watts cautery (Pig TC1) died suddenly 7 days after cautery. Autopsy showed that the pig had 34% tracheal stenosis. In the other two pigs that received 40 watts cautery (Pig TC2 and TC3), only 31%– 32% stenosis had developed by post-cautery day 7. Repeated cautery (40 watts) was applied to these two pigs on post-cautery day 7. At 2 weeks after the initial cautery and 1 week after repeated cautery, hyperplasic granulation tissue grew in the tracheal wall, leading to significant stenosis (63%–65 %) in these pigs (Figure 3 and Table 1).

Figure 3. Tracheal cautery (TC) group. More than one cautery was needed to induce tracheal stenosis.

a. On day 0, 40 watts cautery was performed on Pig TC2.

b. On day 7 in Pig TC2, stenosis was not significant (32%), therefore, repeated cautery was performed.

c. On day 14 in Pig TC2, significant stenosis (65%) had developed as a result of granulation tissue hyperplasia.

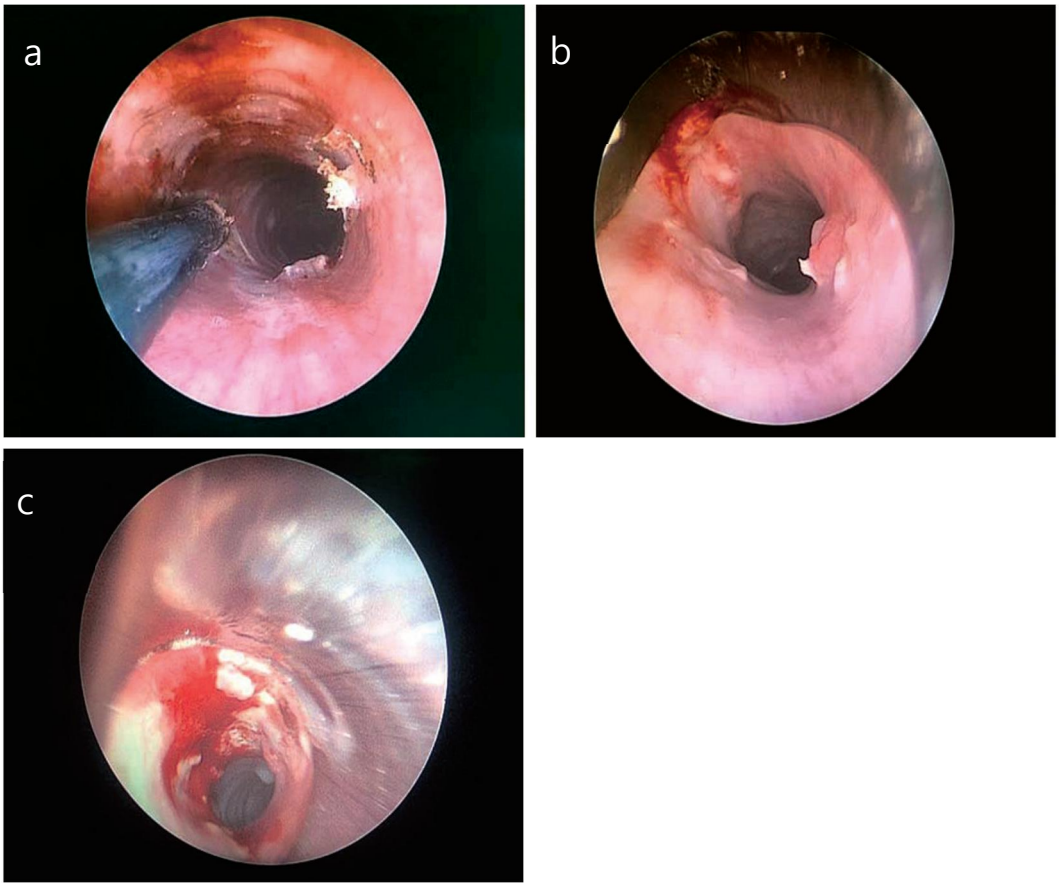

COI Group

In the COI group (Pig COI1, COI2, and COI3), 8-h prolonged intubation was performed with cuff overpressures of 200, 400, and 500 mmHg, respectively. Immediately after prolonged intubation with cuff overpressure, the tracheal mucosa showed redness and sloughing. These ischemia-induced mucosal changes were increased with higher cuff pressures. However, no significant tracheal stenosis occurred during the 2 weeks after intervention (Figure 4 and Table 1).

Figure 4. Cuff overpressure intubation (COI) group. The higher the cuff-pressure, the greater the mucosal change (redness and sloughing) that was noted as reflected by the ischemia induced inflammatory reaction. However, these mucosal changes were not followed by tracheal stenosis.

a. on day 0 in Pig COI1, before COI

b. on day 0, immediately after 8-h 200 mmHg COI.

c. on day 0 in Pig COI2, immediately after 8-h 400 mmHg COI

d. on day 0 in Pig COI3, immediately after 8-h 500 mmHg COI

e. On day 7 in Pig COI3, significant stenosis had not developed (12%).

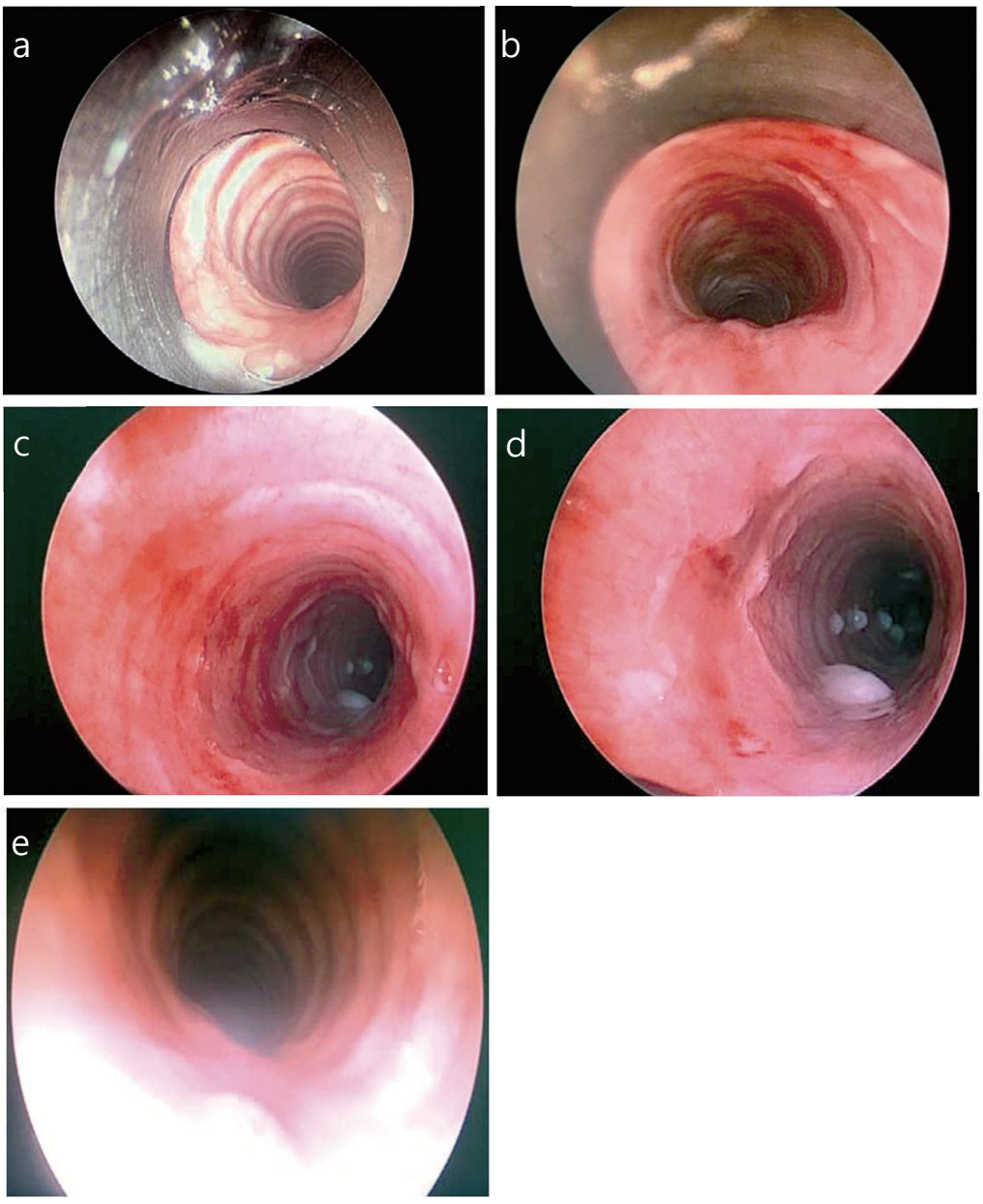

COI-TC Group

In the COI-TC group, eight pigs were divided into three subgroups according to the degree of cuff overpressure: two (Pig COI-TC1 and COI-TC2) at 500 mmHg, four (Pig COI-TC3– COI-TC6) at 400 mmHg, and two (Pig COI-TC7 and COI-TC8) at 200 mmHg. In the 500-mmHg subgroup, two pigs (Pig COI-TC1 and COI-TC2) underwent 8 and 4 h prolonged intubation, respectively. In the 400-mmHg subgroup, four pigs (Pig COI-TC3–COI-TC6) underwent 4, 2, 1, and 0.5 h prolonged intubation, respectively. In the 200-mmHg subgroup, two pigs (Pig COI-TC7 and COI-TC8) underwent 1 and 0.5 h prolonged intubation, respectively. After COI, 40 watts cautery was performed on the tracheal mucosa where the cuff was located.

In the 500-mmHg subgroup, one pig (Pig COI-TC1, 8-h intubation) died suddenly 7 days after COI-TC. Autopsy showed that the pig had 89% tracheal stenosis. Another pig (Pig COI-TC2, 4-h intubation) in this subgroup showed 83% stenosis and 88% stenosis 7 and 14 days after COI-TC, respectively (Figure 5a). The pig was euthanized because of severe dyspnea accompanying costal retraction (Table 1). In the 400-mmHg subgroup, all the pigs (Pig COI-TC3–COI-TC6, 0.5–4-h intubation) showed significant stenosis (53%–80%) 7 days after COI-TC (Figure 5b). The degree of stenosis was proportional to the tracheal intubation time. At 14 days after COI-TC, the stenoses were similar or slightly increased (61%–85%). Pig COI-TC3 and COI-TC4 were euthanized before 21 days because of severe dyspnea accompanying costal retraction (Table 1).

In the 200-mmHg subgroup, one pig (Pig COI-TC7, 1-h intubation) showed 50% stenosis and 58% stenosis 7 and 14 days after COI-TC, respectively (Figure 5c). The other pig (Pig COI-TC8, 0.5-h intubation) in this subgroup showed no significant tracheal stenosis during 2 weeks after intervention (Table 1). Figure 6 shows the histologic findings from Pig COI-TC1 after 7 days of intervention. Severe hyperplasia of granulation tissue and inflammation of the tracheal wall, including the cartilage, were noted (Figure 6).

Figure 5. COI-TC group

The combination of prolonged cuff overpressure intubation (COI) and tracheal injury (tracheal cautery, TC) allows rapid establishment of tracheal stenosis. Tracheal stenosis was increased in proportion to the cuff pressure and tracheal intubation time.

a. On day 7 in Pig COI-TC2, significant stenosis (83%) was noted.

b. On day 7 in Pig COI-TC3, significant stenosis (80%) was noted.

c. On day 7 in Pig COI-TC7, significant stenosis (50%) was noted.

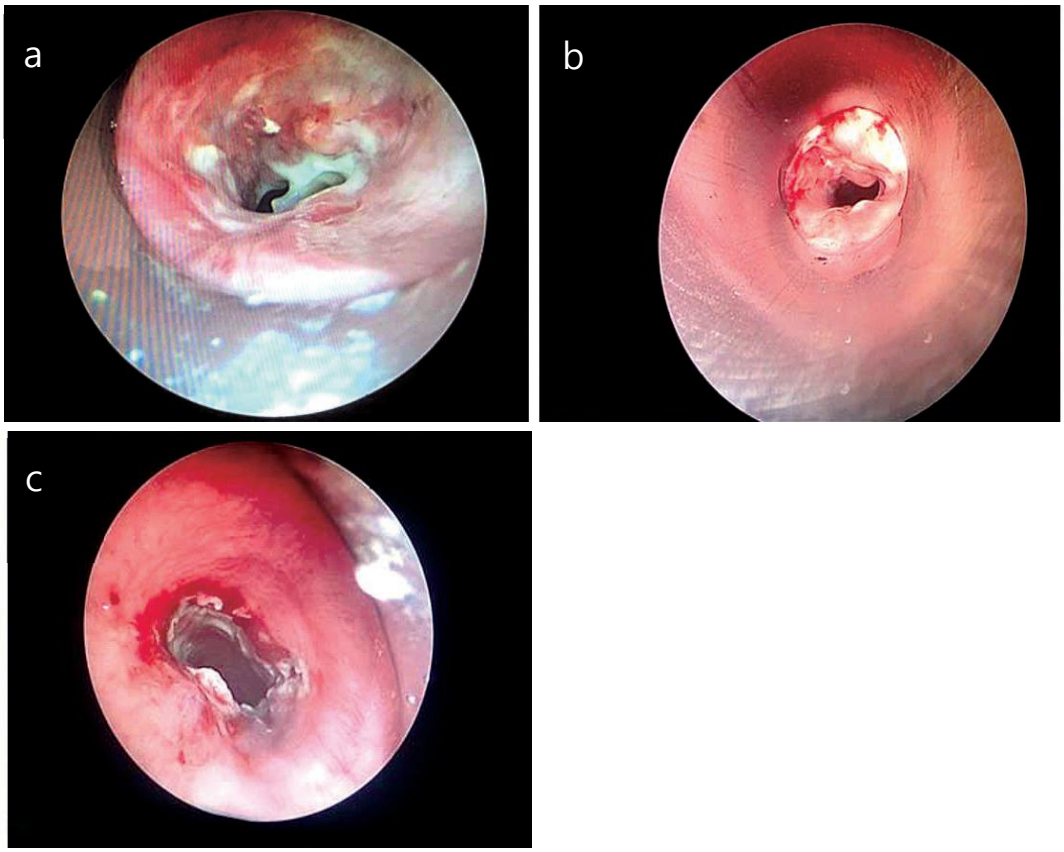

Figure 6. Histologic characteristics of a representative case of COI-TC group (day 7 in Pig COI-TC1)

a. Gross tracheal appearance of a normal segment (left) and stenotic segment (right)

b. Mucosal, submucosal, and cartilaginous structures in the normal tracheal segment (×40)

c. Inflammatory exudate and proliferative granulation tissue in the stenotic tracheal segment (×40)

d. Inflammatory cellular infiltration in the cartilage of the stenotic tracheal segment (×400)

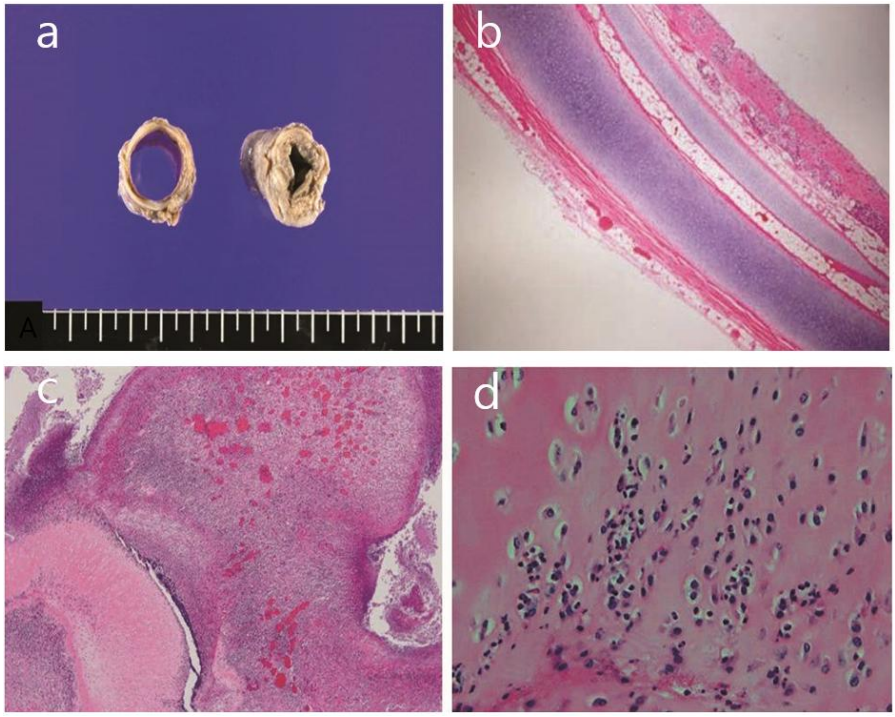

DISCUSSION

This animal study revealed that the combination of COI and tracheal injury (TC) allows rapid establishment of tracheal stenosis in pigs. When the cauterization (40 watts) was performed immediately after over-sized intubation (ID9/OD12) for 1 hour with a cuff pressure of 200 mmHg or more, significant tracheal stenosis occurred in 7 days. In addition, the degree of tracheal stenosis tended to increase in proportion to cuff pressure and tracheal intubation time. This animal model is technically simple and reproducible, and the human tracheal stenosis mechanism is used. This will be of great help in developing new therapies for CAO.

CAO is a possibly life-threatening condition that can be caused by a number of malignant and nonmalignant diseases [2]. The best treatment is surgery; however, this is contraindicated in many cases; therefore, a bronchoscopic treatment, such as an airway stent, is performed. Bronchoscopic treatment is not inherently a complete treatment but rather can lead to complications (e.g., for airway stents: migration, mucostasis, and granulation tissue formation). Therefore it is continuously improving and new treatments are being developed [2-5]. The application of new treatments in humans requires preclinical studies with appropriate animal models. However, previous animal models (dog, pig, and rabbit) of tracheal stenosis take a relatively longer time (3–8 weeks) to develop and require complex processes, and the developmental mechanisms differ somewhat from the actual mechanisms of human tracheal stenosis [6-9]. Human tracheal stenosis is caused by excessive cuff pressure, over-sized intubation, and tracheal damage [10-15]. The present study was conducted to determine how fast tracheal stenosis can be produced by applying the above three mechanisms individually or simultaneously.

In our study, through simultaneous application of COI and TC, successful airway stenosis was induced in seven out of eight pigs (in COI-TC group) within a week. Furthermore, the degree of tracheal stenosis increased in proportion with the cuff pressure and tracheal intubation time. Depending on the degree of cuff overpressure, the minimum required intubation time (immediately before cautery) was different (400 mmHg, 30 min; 200 mmHg, 1 hour). Cuff overpressure alone did not result in significant tracheal stenosis. It did not occur even when the tracheal intubation was maintained for 8 hours at a cuff pressure of 500 mmHg. TC induced airway stenosis, but repeated procedures and a relatively longer time (14 days) were required.

When the cuff pressure is higher than the tracheal capillary pressure (25 mmHg), submucosal blood flow could be impaired, causing ischemic damage to the tracheal wall; for this reason, it is recommended that the cuff pressure for patients maintaining long-term tracheal intubation or tracheostomy does not exceed 25 mmHg [16]. If the cuff pressure is maintained at 100 mmHg for 4 hours, the tracheal cartilage becomes damaged and inflamed [17, 18]. Inflammation of the tracheal wall could induce airway narrowing during the healing process via granulation tissue and fibrotic tissue formation [12, 14, 19]. Su et al produced tracheal stenosis in dogs in a relatively shorter period of time (in 2 weeks) using prolonged intubation with cuff overpressure [20]. Their model required prolonged intubation for at least 24 hours at a cuff pressure of 200 mmHg using an ID7.5 tracheal tube. They did not apply any other manipulation, such as cautery. In our study, 8-hour intubation with a much higher cuff pressure (500 mmHg) did not induce tracheal stenosis. Perhaps, prolonged intubation (long like 24 hours) seems to be more important than cuff overpressure per se in inducing tracheal wall inflammation. However, long-term general anesthesia involves high cost. Sometimes it may not be possible due to the constraints on laboratory operating time, such as in our animal laboratory. We had to find a way to induce tracheal stenosis and the artificial injury (cautery) was attempted in the tracheal mucosa where the cuff pressure was applied.

Electrocautery has been used to induce tracheal stenosis in animals alone or together with other interventions [8, 10]. In this study, stenosis was established in 2–3 weeks. We tried both cautery alone and combined with cuff overpressure. The cautery power was set at 40–60 watts, which is a commonly used range in humans. At 60 watts, however, sudden death occurred with no stenosis induction; accordingly, subsequent experiments were conducted at 40 watts. In our study, to achieve significant tracheal stenosis using cautery alone, two or more sessions of cautery and at least 14 days were needed. In contrast, significant stenosis occurred successfully in 7 days in the cautery plus cuff overpressure combination group. Furthermore, by adjusting the cuff pressure and intubation duration, the degree of stenosis could be predicted. In our opinion, there is a synergistic effect on the induction of tracheal inflammation when both cautery and cuff overpressure intubation are performed simultaneously.

Animal models of airway stenosis are used for the investigation and development of new effective treatments for CAO. To achieve this, the establishment of animal models should not take too long time, and complex or expensive methods are also undesirable. In addition, the degree of induced stenosis can be predicted such that stenosis that is significant but not life-threatening is desirable. Finally, it would be better if it was induced using the same mechanisms leading to human tracheal stenosis. It only takes 7 days to establish our animal model (faster than all previous studies). The method is technically simple and cost effective (induction of tracheal stenosis even with short anesthesia time), and uses the same mechanisms as those underlying human benign tracheal stenosis. In addition, the degree of airway narrowing can be predicted; thus, researchers can induce tracheal stenosis as desired.

The histology of tracheal stenosis in our experiment (COI-TC group) showed acute inflammation of the entire airway wall (including the tracheal cartilage) and granulation tissue overgrowth. Previous studies also have similar histologic findings [15, 21, 22]. Researchers have described that significant tracheal stenosis seems to occur when inflammation of the airway wall spreads to tracheal cartilage beyond the mucosa and submucosa. It seems that cuff overpressure alone did not induce sufficient damage to the tracheal cartilage. In addition, it is presumably thought that COI causes mild fibrosis primarily due to ischemic inflammation. In contrast, heat-induced inflammation by TC is thought to induce granulation tissue formation. By simultaneously applying COI (for fibrosis) and TC (for granulation), it appears that rapid formation of tracheal stenosis was possible.

Our study had some limitations. First, the number of animals in all groups was varied and limited. To generalize our findings, replication studies may be necessary; in particular, detailed validation experiments are required in the COI-TC group, through the experiments, the optimal endotracheal tube size, the optimal intubation duration and cuff pressure, and the optimal cautery energy could be found. Second, there was a lack of results for histological analysis. If the histological analysis was performed more closely according to the group and time point of pigs, we could better identify what is needed to establish tracheal stenosis.

CONCLUSION

Through the present study, we found that the combination of COI and tracheal injury (TC) allows rapid establishment of tracheal stenosis in pigs (within 7 days). In addition, the degree of tracheal stenosis increased in proportion to the cuff pressure and tracheal intubation time. Using this protocol, researchers can induce the desired degree of tracheal stenosis. Establishment of this animal model is technically straightforward and uses mechanisms similar to those underlying human (benign) tracheal stenosis, making it a good experimental tool for developing new therapies for CAO.

PART II

The mechanical characteristics and performance evaluation of a newly developed silicone airway stent (GINA stent)

INTRODUCTION

Although the surgery is the primary treatment for central airway obstruction (CAO), it is limited to certain benign conditions such as post-infection tracheal stenosis, intubation, or tracheostomy due to anatomical limitations, advanced and/or metastatic disease, or poor medical conditions. Eventually, in most cases, CAO can only be resolved by means of bronchoscopic interventions, which frequently require rigid bronchoscopy and include balloon dilatation, mass excision (debulking, debridement), tumor ablation (cryotherapy/argon plasma coagulation/electro-cautery/laser), and stent insertion [23]. Despite the resolution of CAO without using stents is desirable, in reality, the insertion of a stent is the primary technique employed in the treatment of CAO, owing to the cartilage damage in benign stricture or the externally compressive nature of the malignant stricture that occurs in most of the patients with CAO [2, 3] .

Airway stents can be categorized into two main types, each with different characteristics. The metal stent has a substantial expansion (radial) force, which has the advantage of a low migration rate. However, it is associated with a risk of granulation tissue overgrowth and tracheobronchial perforation. Conversely, the silicone stent has a low expansion force, thereby minimizing the risk of granulation tissue overgrowth and tracheobronchial perforation, whereas migration occurs easily. Mucus clogging affects both types of stents [1]. As such, airway stents are effective for immediate relief of CAO but frequently cause complications such as migration, mucostasis, and granulation tissue formation. Consequently, stent technologies are persistently evolving in order to overcome the shortcomings above. The examples include drug-eluting stents (for the inhibition of granulation tissue formation), stents with new designs (for the inhibition of granulation tissue formation/migration), stents with hydrophilic coating on the inner surface (for the inhibition of mucostasis), radiopaque silicone stents, customized three-dimensional (3D) printed stents, and bio-absorbable stents [3-5, 23].

The authors recently developed a new silicone airway stent (named “GINA stent”) based on the anti-migration design, with a flexible, dynamic structure to enable the reduction of stent cross-sectional area, in order to enhance the bronchial expiratory flow, as well as radio-opacity, so that the stent can be easily identified through radio-imaging. The purpose of the present study was to introduce the GINA stent through the assessment of the mechanical properties and quality of

performance in comparison with an established stent, the Dumon stent, via the evaluation of the anti-migration force, expansion force, and flexibility, along with the evaluation of the short-term (3 weeks) performance of the stents using a porcine tracheal stenosis model.

MATERIALS AND METHODS

The GINA stent: a newly developed silicone airway stent.

The GINA stent was fabricated using biocompatible silicone through the process of injection molding. It was intended to have an improved anti-migratory property and maintain airway patency while not exerting excessive force on the airway wall. By referring to the physical (mechanical) properties of the Dumon stent, the target force ranges of the expansion force and flexibility of the GINA stent were set to 10.0–13.5 N and 2.5–4.0 N, respectively, which are slightly lower (but not too low) than the Dumon stent's measurement (N, mean ± SD: 14.54 ± 0.27 and 4.47 ± 0.10, respectively). The target of the friction (anti-migration) force was aimed at more than 13 N, which is higher than that of the Dumon stent (N, mean ± SD, 12.83 ± 0.23) (Table 2). Since the expansion force and flexibility also affect the friction, we tried to ensure that the friction force improvement was achieved through a strategic anti-migratory stent design. By way of repeated stent fabrication and physical measurements, the mixing ratio of silicone, barium, and hardener, and the heating temperature and time were variously modulated. Along with this, the stent surface design was also continuously adjusted. We finally developed a stent that meets our target force ranges.

The GINA stent displayed three specific characteristics. First, the anti-migration design: the outer ring (right-angled triangle shape) of the GINA stent was designed to fit into the cartilaginous trachea; the plane of the stent that comes into contact with the membranous trachea was characterized by a raised, three-line arrangement. Second, a flexible, dynamic structure was considered to facilitate the reduction of the stent cross-sectional area. GINA stent maintains the

physiological airway contraction employing the flat portion of the stent (similar to the membranous portion of the tracheobronchial tree), which renders greater flexibility and facilitates the removal of airway secretions through an enhanced expiratory flow. Third, radio-opacity: barium sulfate was added to the silicone to make the stent radiopaque, so that the stent can be easily identified through radiographic investigations (Figure 7).

In the present study, all the assessments involved the comparison of the GINA stent with the Dumon stent (Novatech, France). A GINA stent with an outer diameter of 14 mm (OD14), ring diameter of 18 mm (RD18), length of 55 mm (L55), and a wall thickness of 1 mm and a Dumon stent with an outer diameter of 14 mm (OD14), surrounding studs of 2 mm (which makes the longest diameter of the Dumon stent 18 mm), length of 50 mm (L50), and a wall thickness of 1.5 mm were selected for the mechanical tests and animal study.

Figure 7. GINA stent, the silicone stent recently developed by the authors, has an anti-migration design, dynamic structure that enables the reduction of stent cross-sectional area, and radio-opacity.

a. Design of the GINA stent.

b. Actual GINA stent [outer diameter of 14 mm (OD14), ring diameter of 18 mm (RD18), and length of 55 mm (L55)].

c. Radio-opacity of the GINA stent.

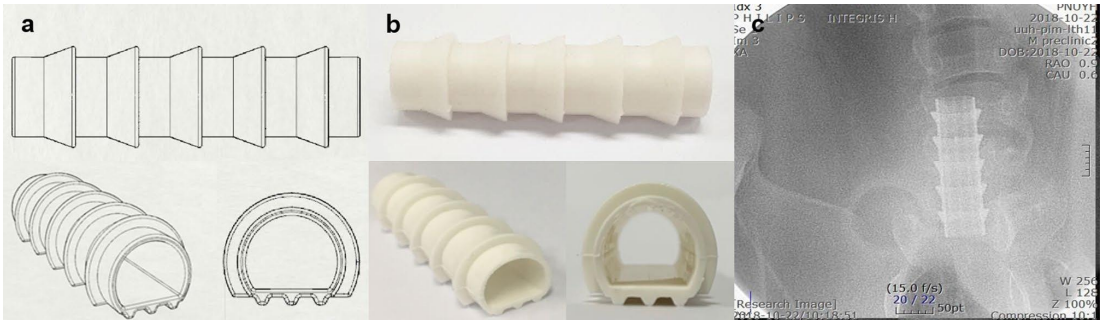

Mechanical tests of the GINA and Dumon stents.

Three mechanical properties (anti-migration force, expansion force, and flexibility), which indicate the actual physiological conditions, were evaluated. The anti-migration force is the frictional force generated between the stent and the airway. In general, the stronger the friction, the lesser the migration [24]. Hence, the frictional force was evaluated to estimate the anti-migration force. The expansion (radial) force is the radial force exerted by the stent on the airway. Flexibility is the elasticity of the stent in response to the external force (i.e., contraction of the airway). Excessive expansion force and low flexibility increase the friction, inducing granulation tissue formation or airway perforation [25-28]. Therefore, to increase the friction, it is desirable to improve the stent design (which could inhibit migration) rather than increase the expansion force or decrease the flexibility. The present study directly evaluated the expansion force and flexibility to assess the risk of granulation tissue formation and airway perforation. All the mechanical tests were performed by the Research and Development Department of the S&G Biotech (Gyeonggido, Korea) [29] using the following methods. The forces were measured using a digital force gauge (LR5K Plus, Lloyd Instruments, Hampshire, England).

The anti-migration force was evaluated using the following method: a Teflon jig with an inner diameter of 16 mm was fixed to the tensile strength tester. Subsequent to the stent insertion into the Teflon jig, a push gauge was used to move the stent to the opposite side of the Teflon jig by 5 cm. Concurrently, the anti-migration force was evaluated (Figure 8a). The average of measurements (n = 5) was considered as the anti-migration force pertaining to each stent. In the case of the GINA stent, the test was performed in both the forward and backward directions.

The expansion force was measured as follows: the stent was positioned on a flat floor. Subsequently, the measuring load cell was attached to the stent surface. The force was measured until the diameter of the stent was reduced by 50% (Figure 8b). The force was measured in various directions (Figure 8d) with tests (n = 5) in each direction and the average of the values was computed. The highest value among the measurements pertaining to different directions was considered as the expansion force of each stent.

The flexibility was evaluated as follows: the measuring jigs were separated at intervals of 4 cm. Subsequently, the stent was placed on the jigs and the measuring load cell was attached to the

stent surface. The measuring load cell pushed the stent slowly and proceeded to half the diameter of the stent. The force was measured according to the advancement of the measuring load cell (Figure 8c). The measurements were made in various directions (Figure 8d) with tests (n = 5) in each direction and the average of the values was computed. The lowest value among the measurements pertaining to different directions was considered as the flexibility of each stent.

Figure 8. The methods used in the mechanical tests. The present study evaluated three mechanical properties (anti-migration force, expansion force, and flexibility) of the GINA and Dumon stents by means of a digital force gauge.

a. The anti-migration force was measured by pushing (5 cm) the stent through a Teflon jig. In the GINA stent, the test was performed in both the forward and backward directions.

b. The expansion force was evaluated by pushing the stent on a flat surface until the stent diameter was reduced by 50%.

c. flexibility was assessed by placing the stent on separate jigs and pushing it by half the diameter of the stent.

d. The arrows indicate the different directions pertaining to the measurements of expansion force and flexibility.

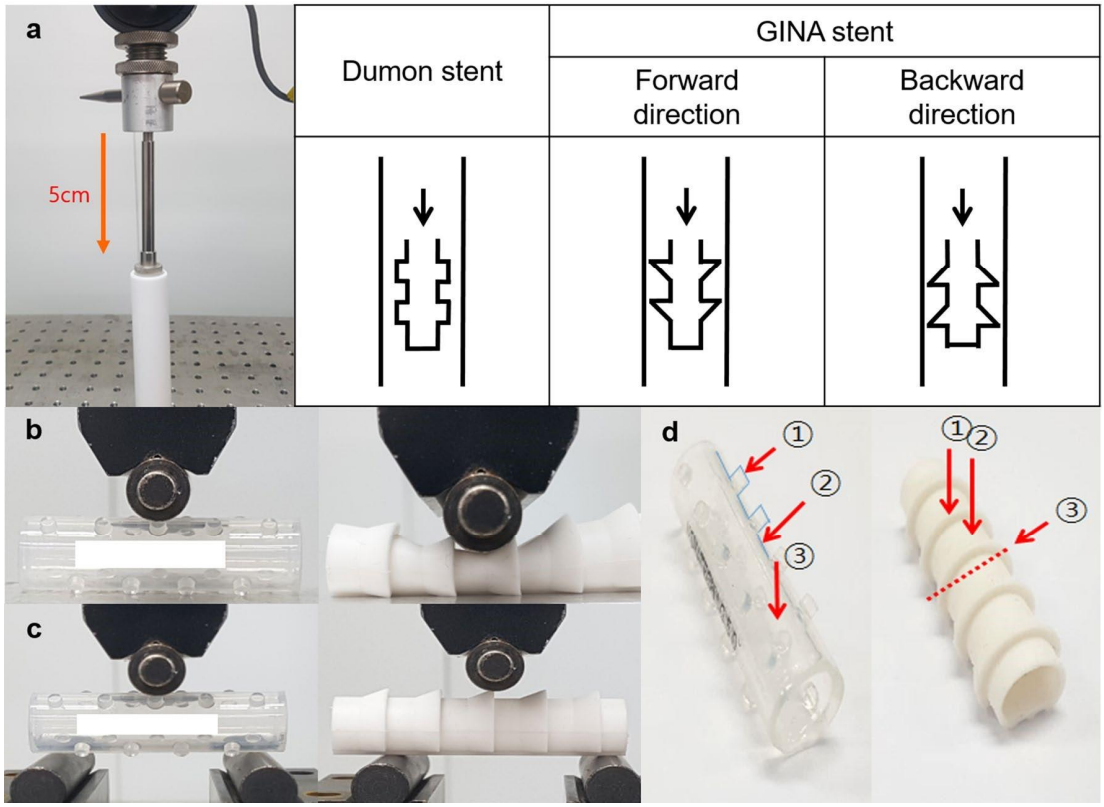

Evaluation of the performance of GINA and Dumon stents in animal models.

The present study assessed the GINA stent's short-term (3 weeks) performance, compared to the Dumon stent, using a porcine model of tracheal stenosis. In order to perform this experiment, seven 12-week-old, female farm pigs (body weight: 40–45 kg) were selected, on account of the similarity between the porcine and adult human tracheal diameters (16–20 mm).

Tracheal stenosis was induced 5 cm below the vocal cords using the methods of cuff overpressure intubation (COI) and tracheal cautery (TC), which were recently developed by the authors [30]. Momentarily, 200 mmHg of COI was applied to the porcine trachea by means of a silicone tracheal tube (internal diameter (ID): 9.0 mm; outer diameter (OD): 12 mm) for a duration of one hour. Subsequently, the tracheal mucosa in the region of the location of the cuff was cauterized [40 W by coagulation suction tube (10390 BN, Karl Storz, Germany)] by means of a rigid bronchoscope (size 8.5, 10318 BP, Karl Storz, Germany) (Figure 9a). After 7 days of COI and TC, the induction of tracheal stenosis was confirmed by a $\geq 50\%$ reduction in the measured airway cross-sectional area (Figure 9b) and the stent insertion was performed.

Four received the GINA stent among the seven pigs and three received the Dumon stent (Figure 9c, d). A TONN/NOVATECH stent applicator (Novatech, France) was used to position the stents using a rigid bronchoscope (size 14, 10318 GL, Karl Storz, Germany). The stent performance was assessed using flexible bronchoscopy (MAF-TM, Olympus, Tokyo, Japan) every week for three weeks after the stent insertion. The performance evaluation involved the examination of the stents to assess migration, granulation tissue overgrowth at both ends, and mucostasis.

In the present study, intramuscular alfaxan (5 mg/kg) and inhalational 3% isoflurane were used to induce and maintain general anesthesia, respectively. All the experimental animals were handled in accordance with well-established bioethical guidelines (Guiding Principles in the Care and Use of Animals, DHEW Publication, NIH). The present study followed the protocol approved by the Institutional Animal Care and Use Committee of the Pusan National University Yangsan Hospital (Approval Number: PNUYH-2017-043), and was in compliance with the ARRIVE (Animal Research: Reporting of In Vivo Experiments) guidelines.

Figure 9. Evaluation of the performance of the GINA stent, compared to the Dumon stent, using porcine tracheal stenosis models. After inducing tracheal stenosis in 12-week-old pigs, a stent (GINA or Dumon) was inserted and the animals were observed for a time period 3 weeks.

a. The induction of stenosis (5 cm below the vocal cords) by means of cuff overpressure intubation and subsequent tracheal cautery.

b. Induced tracheal stenosis (a reduction in the measured airway cross-sectional area by at least 50%).

c, d. The GINA and Dumon stents inserted into the stenotic porcine tracheae.

e, f. The GINA and Dumon stents after 21 days.

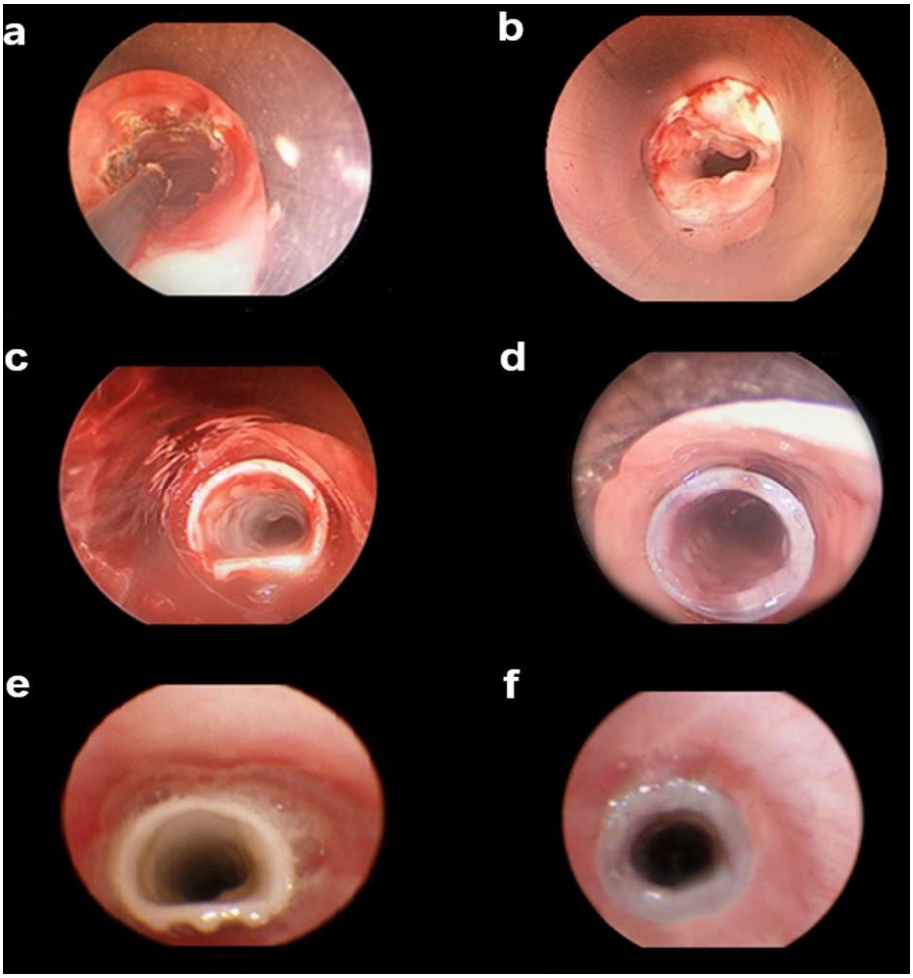

Statistical analysis.

The null hypothesis regarding the mechanical properties (anti-migration force, expansion force, and flexibility) was that there was no difference in the measurements between the two types of stents. The null hypothesis regarding the performance (migration, granulation tissue formation, and mucus retention) in a porcine model was that there was no difference in the incidences between the two types of stents. Statistical analyses were performed using SPSS 21 (IBM, Chicago, Illinois, USA). Because of the non-normal distribution and small numbers available for analyses, the Mann–Whitney U test (for continuous variables) and Fisher's exact test (for dichotomous variables) were used to identify any potential associations. A P value < 0.05 was considered statistically significant in all analyses.

RESULTS

Mechanical characteristics of the GINA stent.

The anti-migration forces are illustrated in Figure 10a and Table 2. The GINA stent displayed stronger anti-migration forces in both directions, compared to the Dumon stent [Newton (N), mean ± Standard deviation (SD): Dumon stent, 12.83 ± 0.23 vs. GINA stent, 15.21 ± 0.59 (in the forward direction) and 18.4 ± 0.51 (in the backward direction), P = 0.008]. The stronger the anti-migration force, the lower the probability of stent migration, thereby minimizing the inherent complications associated with the stent.

The GINA stent displayed a lower expansion force, compared to the Dumon stent (N, mean ± SD: 11.91 ± 0.21 vs. 14.54 ± 0.27 N, P = 0.008) (Figure 10b and Table 2). Additionally, in terms of the stent flexibility, the GINA stent required a lower force to flex the stent, compared to the Dumon stent (N, mean ± SD: 3.13 ± 0.06 vs. 4.47 ± 0.10, P = 0.008) (Figure 10c and Table 2). Low expansion force and high flexibility can reduce the risk of granulation tissue formation and

airway perforation. The results of the mechanical tests indicate that the GINA stent has superior mechanical properties, compared to the Dumon stent.

Figure 10. The results pertaining to the mechanical tests.

a. The GINA stent displayed stronger anti-migration force in both directions, Compared to the Dumon stent.

b-c. The GINA stent displayed lower expansion force and higher flexibility. *N* Newton.

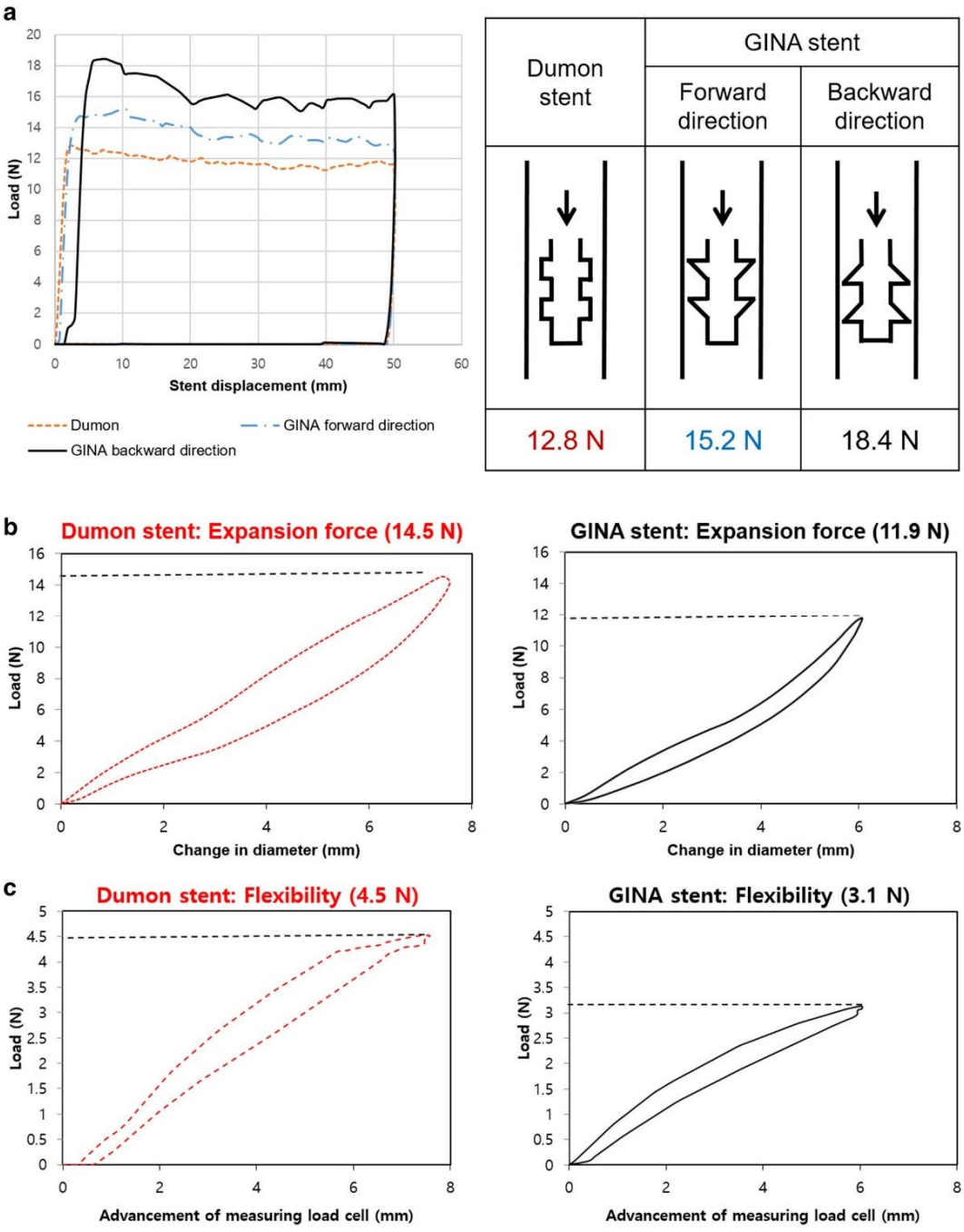

Table 2. Detailed results of the mechanical tests

Measurement No.	Anti-migration force (N)			Expansion force (N)						Flexibility (N)					
	Dumon	GINA forward	GINA backward	Dumon ①	Dumon ②	Dumon ③	GINA ①	GINA ②	GINA ③	Dumon ①	Dumon ②	Dumon ③	GINA ①	GINA ②	GINA ③
	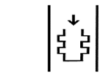														
1	12.91	15.62	18.71	6.04	6.85	14.41	10.10	12.20	8.74	4.42	4.87	7.57	3.15	4.29	5.98
2	12.69	14.68	18.92	6.04	6.81	14.32	10.16	11.95	8.76	4.38	4.95	7.59	3.06	4.45	5.18
3	12.90	14.52	18.75	5.98	6.82	14.85	10.16	11.82	8.87	4.39	4.97	7.46	3.09	4.41	5.30
4	12.53	15.32	17.94	6.01	6.78	14.29	10.50	11.62	8.72	4.61	4.83	7.54	3.18	4.33	5.85
5	13.13	15.90	17.80	6.05	6.91	14.82	10.40	11.94	7.85	4.55	4.91	7.44	3.19	4.20	5.31
Mean	12.83	15.21	18.42	6.02	6.83	14.54	10.26	11.91	8.59	4.47	4.91	7.52	3.13	4.34	5.52
Standard deviation	0.23	0.59	0.51	0.03	0.05	0.27	0.18	0.21	0.42	0.10	0.06	0.07	0.06	0.10	0.36
P-value		0.008 (compared to Dumon)	0.008 (compared to Dumon)				0.008 (compared to Dumon ③)						0.008 (compared to Dumon ①)		

Abbreviation: N, Newton

Performance of the GINA stent in a porcine model.

The results of the evaluation of short-term (3 weeks) performance of the GINA stent, compared to the Dumon stent, in a porcine model of tracheal stenosis are summarized in Table 3. Stent migration was detected on the fourteenth day after stent implantation in one of the four pigs that underwent GINA stent insertion. Among the three pigs that underwent Dumon stent insertion, stent migration was detected on the seventh and fourteenth day after stent insertion in two pigs. All the stent migrations were observed to be proximal migrations that were completely expelled from the body. Mucus retention and granulation tissue formation were not detected in either of the two types of stents during the 3 weeks after insertion (Figure 9e, f).

Table 3. Short-term (3 weeks) performance of the GINA stent, compared to the Dumon stent, in a porcine model of tracheal stenosis. *P = 0.486 for GINA versus Dumon.

Pig no.	Inner diameter of trachea on day 0 (mm)	Inner diameter of trachea on day 7, mm	Stenosis, %	Stent	Migration*	Time interval between stent insertion and migration, days	Mucus retention	Granulation tissue formation at both ends
1	17	11	58	GINA	No	–	No	No
2	18	12	56	GINA	No	–	No	No
3	16	10	61	GINA	Yes (proximal)	14	No	No
4	17	11	58	GINA	No	–	No	No
5	16	11	53	Dumon	Yes (proximal)	7	No	No
6	16	10	61	Dumon	Yes (proximal)	14	No	No
7	17	12	50	Dumon	No	–	No	No

DISCUSSION

GINA stent, a radiopaque silicone airway stent that was recently developed by the authors, was designed to minimize migration, mucostasis, and granulation tissue formation. The mechanical tests performed in the current study confirmed that the GINA stent has a lower possibility of migration and granulation tissue formation, compared to the Dumon stent. Moreover, the results of the performance evaluation using porcine models suggest that the performance of the GINA stent is not inferior to that of the Dumon stent.

The conditions regarding an ideal airway stent are cost-effectiveness, ease of insertion and removal, devoid of migration or granulation tissue formation, not excessive but adequate expansion force against airway stenosis, adequate flexibility to preserve the airway physiology, and without any impairment of the mucociliary clearance [25]. However, no stent is capable of fulfilling all of the aforementioned conditions; if one characteristic is superior, another tends to be inferior. For instance, if the stent has low expansion force and the likelihood of granulation Accordingly, metal stents have a low migration rate, but a high rate of granulation tissue formation, whereas silicone stents have a high migration rate, but a low rate of granulation tissue formation1. In terms of the inhibition of mucostasis in the stent, it is desirable to maintain the mucociliary clearance, and necessary to be flexible so that the stent inner diameter is sufficiently reduced during exhalation. The uncovered metal stent could best preserve the mucociliary clearance. However, removal of the stent is difficult, owing to epithelialization, in addition to the problem of tissue ingrowth within the stent. Consequently, an uncovered metal stent is not recommended for the management of benign airway stenosis; the use is restricted to the palliation of malignant airway stenosis, but tumor ingrowth should be a concern [26]. After all, improving the flexibility of the stent (enabling the reduction of stent cross-sectional area) is the most rational method of resolving mucostasis, thereby facilitating the removal of airway secretions through the enhanced expiratory flow.

In the present study, the GINA stent showed a lower expansion force and higher flexibility, compared to the Dumon stent. Although the current study did not observe any substantial difference between the two types of stents with regard to the formation of granulation tissue in the porcine models, it could be attributed to the short observation period. Granulation tissue

formation is a common complication of silicone airway stents, although less than in metal s tents [1, 2, 27]. Excessive expansion force and low flexibility are the predisposing factors associated with granulation tissue formation [27, 28, 31, 32]. The low expansion force and high flexibility of the GINA stent implies that less force is required to expand and bend the stent, resulting in less pressure on the airway, leading to diminished mucosal inflammation and granulation tissue formation.

Despite the low expansion force, the GINA stent displayed a higher anti-migration force, compared to the Dumon stent, which was further confirmed by the animal experiments. The aforesaid superiority can be attributed to the creative surface design of the GINA stent, which comprises a right-angled triangle-shaped outer ring pertaining to the cartilaginous trachea and a raised, three-line arrangement pertaining to the membranous trachea. During the formulation of the design of the GINA stent, we reviewed several previously developed airway stents and the most inspiring were the Freitag stent and the Natural stent [6, 33, 34]. The two aforementioned stents have a common outer ring for cartilaginous trachea, which plays a role in the inhibition of migration. The current design improved on this feature (to maximize the anti-migratory friction) by transforming the outer ring into a right-angled triangle shape, and including a raised, three-line arrangement for the membranous trachea. The right-angled triangle-shaped outer ring is specifically designed to further suppress the proximal migration of the stent, which is more dangerous, compared to distal migration (proximal migration can lead to glottic obstruction or complete stent breakaway, resulting in suffocation) [35, 36]. The present study confirmed this through the results of the mechanical test, which showed an improved anti-migration force in relation to the GINA stent backward direction. Moreover, the in-vivo effectiveness was recognized to a certain extent through the evaluation of short-term performance. Migration is a common complication associated with airway stents, especially silicone stent [37, 38], and several attempts have been made to inhibit the same. The Montgomery T tube was fabricated with a side arm that passes through a tracheostomy, which provides the stent with a fixation to the trachea [39]. Recently, an external fixation method was introduced, which resolved the cosmetic problem associated with the Montgomery T tube [40]. However, these methods can only be employed for the management of upper tracheal stenosis. In case of lower tracheal or bronchial stenosis, a bifurcation stent might facilitate the prevention of migration. However, the stent insertion is a

challenging endeavor, owing to the size of the stent, which is excessively large, compared to the segment of stenosis [41, 42]. Nevertheless, in order to prevent the migration of the stent, it is necessary to improve the friction (i.e., anti-migration force) using stents of suitable dimensions [diameter larger than the stenosis, but slightly smaller (80–90%), compared to the airway diameter around the stenosis] [2, 43] as well as by improving the stent surface design (like studs, spikes, or protruding arcs) [5, 35, 40, 44, 45].

Another important feature of the GINA stent is the flexible, dynamic structure, which enables the reduction of the stent cross-sectional area. The GINA stent has a flat part, similar to the membranous portion of the actual tracheobronchial tree, which makes the stent more contractible and facilitates the removal of airway secretions through an enhanced expiratory flow. Freitag and Kim have already demonstrated that flattening a part of the stent improves the mucostasis [6, 33, 34, 46]. The current performance study did not observe any substantial difference between the two types of stents with regard to the mucostasis, which might be ascribed to the short observational period.

Lastly, the GINA stent is radiopaque, which makes stent-tracking easier. The radiolucency of silicone stents (such as Dumon stents) has been considered to be a major drawback and efforts have been made to improve the same. Recently, a radiopaque version of the Dumon stent was developed.

Despite the success associated with the development of the GINA stent, the current study does not preclude limitations. First, the sample size of the animals that were involved in the experimental evaluation of the performance of the stents was small and the duration of observation was short. The current study did not observe any substantial difference between the two types of stents with regard to the mucus retention and granulation tissue formation, which is presumed to be due to the short duration of the experiment. The current study observed a difference between the two types of stents with reference to migration. However, it was not statistically significant, on account of the small sample size. Second, the current study did not compare the histology of the tissues at the sites of stent insertion. However, a follow-up study to ascertain the difference between the two types of stents with regard to the degree of injury at the site of stent insertion will be planned in the future. Third, the current study performed the

mechanical tests on the basis of the advice provided by the stent manufacturing company (S&G Biotech, Gyeonggi-do, Korea) and previous studies [5, 47, 48]. Due to the lack of a validated method, existing studies have used simple or complex methods according to the nature and requirements of the respective studies. Consequently, the authors were compelled to conduct the experiments in a selective manner, in accordance with the laboratory conditions. For instance, it is more desirable to assess the anti-migration force using ex-vivo tracheal tissue or the materials that mimic the same, but we could not. Therefore, the current results should be interpreted with due consideration of the limitations.

CONCLUSION

In conclusion, the authors have developed a new stent through strategic design, which has reduced migration, despite the low expansion force and increased flexibility, in order to reduce the likelihood of granulation tissue formation. The scenario warrants future clinical trials to demonstrate the efficacy and safety of GINA stents in humans.

PART III

3D-engineered personalized airway stent (custom GINA stent): introduction and performance evaluation in pigs

INTRODUCTION

Treating complex airway stenosis is often not easy for conventional ready-made stents. In addition, conventional stents have significant drawbacks, such as migration, mucostasis, and granulation tissue formation, which can result in stent malfunction and even life-threatening. Recently, custom stents have been introducing to overcome these obstacles. Thanks to the rapid development of 3D printing technology, intricate structures can be efficiently created at low cost in a short time. However, reports on the development of custom stents using 3D technology are limited, and the stent design itself focuses only on the shape of the airway [49-51].

We previously developed a GINA stent with a new design and confirmed that it performs better than the Dumon stent in terms of its mechanical properties and in animal model experiments [52]. The GINA stent improved the anti-migration design using right-angled triangle-shaped outer rings for the cartilaginous trachea and a raised, three-line arrangement for the membranous trachea; tried to maintain the airway's physiological role with a flexible and dynamic structure though using a flat part, similar to the membranous portion of the tracheobronchial tree; and added a radiopaque material to check positioning more easily. This study developed a 3D-engineered personalized airway stent that hybridized the GINA stent design and evaluated its short-term performance in a pig model of tracheal stenosis. Pigs were chosen as the animal model because their tracheal size is similar to that of humans, and because the tracheal bronchus originates before both main stem bronchi, it is possible to experiment with complex airway stenosis. We named our 3D-engineered personalized airway stent the “custom GINA stent”. Here, we report a novel use of 3D-engineered custom airway stents for tracheal stenosis in animal models.

MATERIALS AND METHODS

Stent fabrication process

First, we obtained a computed tomography (CT) scan of a pig. Using the 3D slicer Mimics software (Materialize, Belgium), we selected and cut out the airway area of interest to create a 3D airway model. We then applied the GINA stent design to the 3D model using the Rhino computer-aided design (CAD) program (Robert McNeel, Seattle, WA, USA). After saving stent modeling as a standard for the exchange of product files, we used a computer numerical control machine to produce the mold. The stent was made of a silicone mixture (biocompatible medical-grade silicone, hardener, and barium) using injection molding. The injected mold was then treated at 70 for 140 min. When the silicone mixture hardened, the mold was removed, and the surfaces were polished (Figure 11a).

Figure 11. 3D-engineered personalized stent (custom GINA stent) and performance evaluation in a pig tracheal stenosis model.

(a) The custom GINA stent was planned using computer-aided 3D design based on computed tomography (CT) scan data and fabricated using a 3D-engineered mold.

(b) Lower trachea (before inducing stenosis) with a tracheal bronchus and both main stem bronchi in the first pig.

(c) The first pig was cauterized on days 0 and 7 to induce stenosis.

(d) Approximately 75% tracheal stenosis was induced in the first pig by day 14.

(e) The custom GINA stent was implanted using rigid bronchoscopy in the first pig on day 16.

(f) X-ray showing that the custom GINA stent was in situ in the first pig on day 37 (stent day 21).

(g) CT scan showing that the custom GINA stent was in situ in the first pig on day 37 (stent day 21).

(h and i) 3D-reconstructed CT scan images with the implanted custom GINA stent in the first pig.

(j) The lower trachea of the second pig was cauterized on days 0 and 3 to induce stenosis.

(k and l) Before and after induction of tracheal stenosis; 63% tracheal stenosis was observed on 3D-reconstructed CT scan images in the second pig on day 7.

(m) The custom GINA stent was implanted using rigid bronchoscopy in the second pig on day 7.

(n) X-ray showing that the custom GINA stent was in place in the second pig on day 28 (stent day 21).

(o) CT scan showing that the custom GINA stent was in place in the second pig on day 28 (stent day 21).

(p and q) 3D-reconstructed CT scan images with implanted custom GINA stent in the second pig.

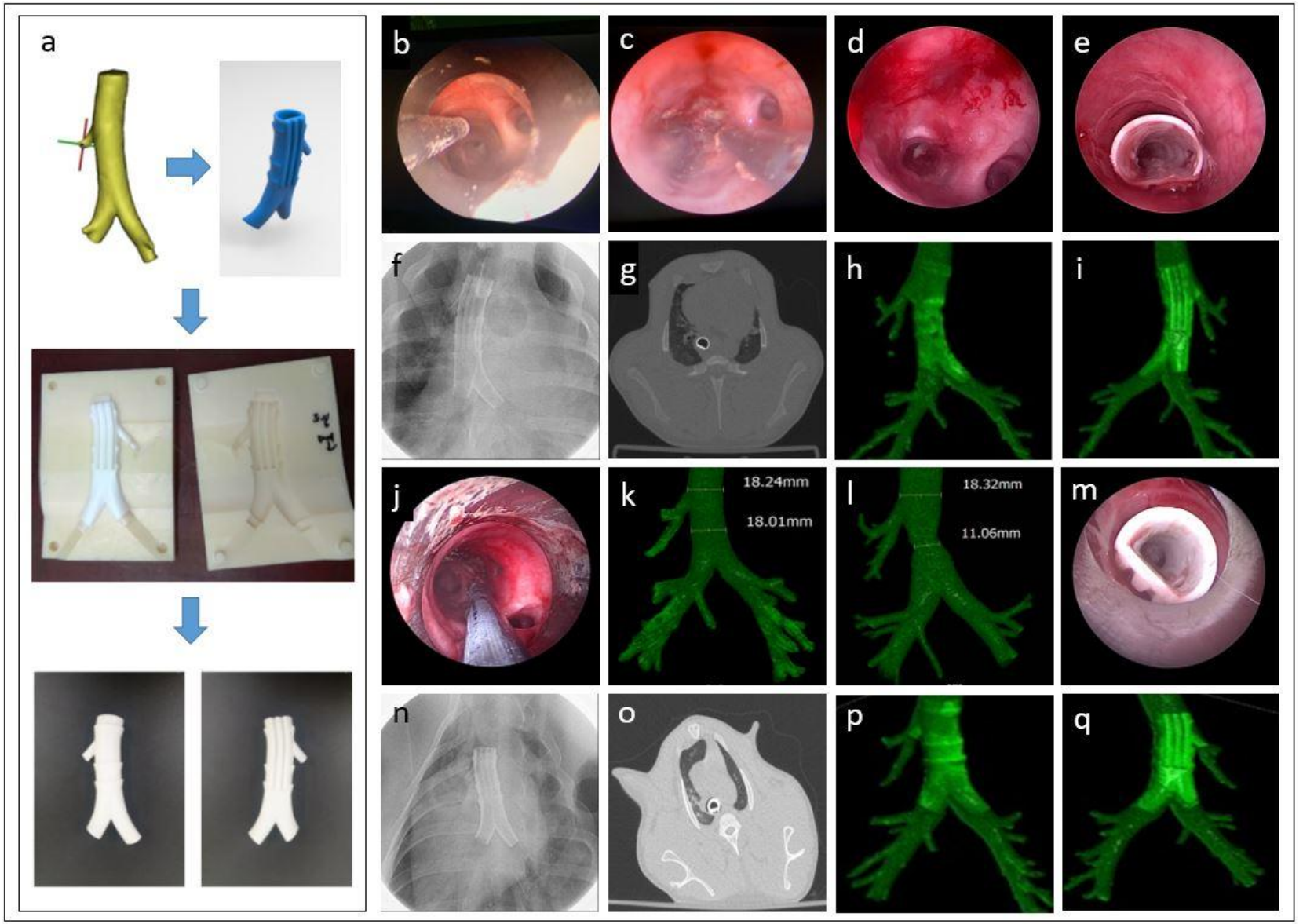
a
b
c
d
e
f
g
h
i
j
k
18.24mm
18.01mm
l
18.32mm
11.06mm
m
n
o
p
q

Performance evaluation of custom stent

The performance of the stent was tested in a swine tracheal stenosis model previously developed by our group in two pigs [30]. On the first day, baseline CT was performed, and a stent was fabricated based on the CT data; stenosis induction (tracheal cautery) was performed on the same day. X-ray, CT, and flexible bronchoscopy (MAF-TM; Olympus, Tokyo, Japan) were performed every week after stenosis induction until the end of the experiment. If the stenosis was more than 50% and the stent fabrication was complete, rigid bronchoscopy (Karl Storz, Germany) was performed to implant a custom GINA stent into the pig. After stent implantation, the pigs were observed for an additional three weeks.

RESULTS

In the first pig, the stenosis was 25% on day 7; therefore, cautery was applied once more. At two weeks, 75% stenosis was observed. Stent fabrication was completed on the 16th day, and stent implantation was performed on the same day. Three weeks after stent insertion, it remained in situ, and neither granulation tissue formation at either end nor mucostasis was observed (Figure 11b–11i). In the second pig, two cauteries (3-day interval) were performed in the first 3 days to promote stenosis. At one week, the stenosis rate was 63%. Stent fabrication was completed on the 7th day after obtaining the baseline CT, and the stent was inserted at the same time. We observed the pig for three weeks after the insertion; similar observations to those in the first pig were also seen in the second pig (Figure 11j ~ 11q).

DISCUSSION

With existing ready-made stents, migration and granulation tissue formation are not uncommon because a distorted airway structure is not considered. With recent developments in technology

and cost reduction, it is thought that stent production using CAD and 3D printing can overcome these shortcomings. This study produced a 3D-engineered personalized airway stent (custom GINA stent) rapidly (in 7 days) and evaluated its short-term performance in an animal model. What distinguishes our stent from other custom stents is that the creative GINA stent design was applied to the custom stent [4]. Right-angled triangle-shaped outer rings and raised three-line arrangements were added to the stent outer wall to increase friction. A flat part, similar to the membranous portion of the human trachea, was included in the design to make the stent more contractible when exhaling. This action enhances expiratory flow and prevents mucostasis.

The human application of 3D customized stents has already been attempted several years ago [49-51], therefore the value of our study conducted only in animals is limited. In addition, the use of two pigs was insufficient to prove the efficacy and safety of this approach. Therefore, we wish this as a study to highlight the plausibility of this treatment. Even using the same type (silicone) of custom stent, there may be differences in performance depending on the physical properties or design of the stent; therefore, it is desirable to check the performance in animal experiments before application in humans.

CONCLUSION

In conclusion, we developed a personalized airway stent with a novel design using 3D engineering within 7 days, and the short-term stent performance was evaluated. This approach will contribute to the shift from ready-made stents to personalized stents.

REFERENCES

1. Ernst, A. and F.J.F. Herth, *Principles and Practice of Interventional Pulmonology*. 2012: Springer New York.

2. Flannery, A., et al., *The Art of Rigid Bronchoscopy and Airway Stenting.* Clin Chest Med, 2018. **39**(1): p. 149-167.

3. Herth, F.J. and R. Eberhardt, *Airway stent: what is new and what should be discarded.* Curr Opin Pulm Med, 2016. **22**(3): p. 252-6.

4. Kwon, C.I., et al., *Bile Flow Phantom Model and Animal Bile Duct Dilation Model for Evaluating Biliary Plastic Stents with Advanced Hydrophilic Coating.* Gut Liver, 2016. **10**(4): p. 632-41.

5. Xavier, R.G., et al., *[Development of a modified Dumon stent for tracheal applications: an experimental study in dogs].* J Bras Pneumol, 2008. **34**(1): p. 21-6.

6. Kim, H.J., et al., *The Usefulness and Safety of Natural Stent in a Canine Model of Tracheal Stenosis.* Tuberc Respir Dis KUID - 1003TRD/2002.53.4.431, 2002. **53**(4): p. 431-438.

7. Lee, H.S., et al., *Rabbit model of tracheal stenosis induced by prolonged endotracheal intubation using a segmented tube.* Int J Pediatr Otorhinolaryngol, 2015. **79**(12): p. 2384-8.

8. Lee, S.S., et al., *A new model of tracheal stenosis in dogs using combined bronchoscopic electrocautery and ethanol injection.* J Vasc Interv Radiol, 2008. **19**(5): p. 764-9.

9. Marquette, C.H., et al., *Experimental models of tracheobronchial stenoses: a useful tool for evaluating airway stents.* Ann Thorac Surg, 1995. **60**(3): p. 651-6.

10. Eliashar, R., et al., *Improved canine model for laryngotracheal stenosis.* Otolaryngol Head Neck Surg, 2000. **122**(1): p. 84-90.

11. Halum, S.L., et al., *A multi-institutional analysis of tracheotomy complications.* Laryngoscope, 2012. **122**(1): p. 38-45.

12. Li, M., et al., *Risk Factors for Posttracheostomy Tracheal Stenosis.* Otolaryngol Head Neck Surg, 2018. **159**(4): p. 698-704.

13. Liu, J., et al., *Post-intubation tracheal stenosis after management of complicated aortic dissection: a case series.* J Cardiothorac Surg, 2015. **10**: p. 148.

14. Vandemoortele, T., et al., *Endobronchial treatment of complete tracheal stenosis: report of 3 cases and description of an innovative technique.* Ann Thorac Surg, 2013. **95**(1): p. 351-4.

15. Wain, J.C., Jr., *Postintubation tracheal stenosis.* Semin Thorac Cardiovasc Surg, 2009. **21**(3): p. 284-9.

16. Marino, P.L., *Marino's the ICU book.* Chapter 28. The Ventilator-Dependent Patient, 2014.

17. Knowlson, G.T. and H.F. Bassett, *The pressures exerted on the trachea by endotracheal inflatable cuffs.* Br J Anaesth, 1970. **42**(10): p. 834-7.

18. Leigh, J.M. and J.P. Maynard, *Pressure on the tracheal mucosa from cuffed tubes.* Br Med J, 1979. **1**(6172): p. 1173-4.

19. Esteller-More, E., et al., *Prognostic factors in laryngotracheal injury following intubation and/or tracheotomy in ICU patients.* Eur Arch Otorhinolaryngol, 2005. **262**(11): p. 880-3.

20. Su, Z., et al., *A canine model of tracheal stenosis induced by cuffed endotracheal intubation.* Sci Rep, 2017. **7**: p. 45357.

21. Jung Kwon, O., et al., *Tracheal stenosis depends on the extent of cartilaginous injury in experimental canine model.* Exp Lung Res, 2003. **29**(6): p. 329-38.

22. Verkindre, C., et al., *Morphological changes induced by extensive endobronchial electrocautery.* Eur Respir J, 1999. **14**(4): p. 796-9.

23. Swami, H., M. Bharath, and B. Chaitra, *Evaluation of management of tracheal stenosis: our experience of 25 patients.* International Journal of Otorhinolaryngology and Head and Neck Surgery, 2016. **2**: p. 174-179.

24. Mozafari, H., et al., *Migration resistance of esophageal stents: The role of stent design.* Comput Biol Med, 2018. **100**: p. 43-49.

25. Guibert, N., et al., *Integration of interventional bronchoscopy in the management of lung cancer.* European Respiratory Review, 2015. **24**(137): p. 378-391.

26. Lemaire, A., et al., *Outcomes of tracheobronchial stents in patients with malignant airway disease.* Ann Thorac Surg, 2005. **80**(2): p. 434-7; discussion 437-8.

27. Murgu, S.D. and H.G. Colt, *Complications of silicone stent insertion in patients with expiratory central airway collapse.* Ann Thorac Surg, 2007. **84**(6): p. 1870-7.

28. Rafanan, A.L. and A.C. Mehta, *Stenting of the tracheobronchial tree.* Radiol Clin North Am, 2000. **38**(2): p. 395-408.

29. Biotech., S.G., www. sngbio. co. kr.

30. Kim, J.H., et al., *Rapid Establishment of Tracheal Stenosis in Pigs Using Endotracheal Tube Cuff Overpressure and Electrocautery.* Curr Med Sci, 2021. **41**(2): p. 329-335.

31. de Mello-Filho, F.V., S.M. Antonio, and R.L. Carrau, *Endoscopically placed expandable metal tracheal stents for the management of complicated tracheal stenosis.* Am J Otolaryngol, 2003. **24**(1): p. 34-40.

32. Folch, E. and C. Keyes, *Airway stents.* Ann Cardiothorac Surg, 2018. **7**(2): p. 273-283.

33. Freitag, L., et al., *Theoretical and experimental basis for the development of a dynamic airway stent.* Eur Respir J, 1994. **7**(11): p. 2038-45.

34. Ryu, Y.J., et al., *Comparison of natural and Dumon airway stents for the management of benign tracheobronchial stenoses.* Respirology, 2006. **11**(6): p. 748-54.

35. Bolliger, C.T., et al., *Evaluation of a new self-expandable silicone stent in an experimental tracheal stenosis.* Chest, 1999. **115**(2): p. 496-501.

36. Madan, M., et al., *Acute Aphonia Following Proximal Migration of a Tracheal Silicone Stent.* J Bronchology Interv Pulmonol, 2021. **28**(1): p. e11-e14.

37. Ernst, A., et al., *Central airway obstruction.* Am J Respir Crit Care Med, 2004. **169**(12): p. 1278-97.

38. Karush, J.M., et al., *Durability of Silicone Airway Stents in the Management of Benign Central Airway Obstruction.* Lung, 2017. **195**(5): p. 601-606.

39. Wahidi, M.M. and A. Ernst, *The Montgomery T-tube tracheal stent.* Clin Chest Med, 2003. **24**(3): p. 437-43.

40. Mehta, R.M., et al., *The "Hitch Stitch": An Effective Method of Preventing Migration in High Tracheal Stenosis.* Respiration, 2017. **93**(2): p. 106-111.

41. Dutau, H., et al., *Use of the Dumon Y-stent in the management of malignant disease involving the carina: a retrospective review of 86 patients.* Chest, 2004. **126**(3): p. 951-8.

42. Oki, M. and H. Saka, *New dedicated bifurcated silicone stent placement for stenosis around the primary right carina.* Chest, 2013. **144**(2): p. 450-455.

43. Hu, H.C., et al., *Granulation tissue formation following Dumon airway stenting: the influence of stent diameter.* Thorac Cardiovasc Surg, 2011. **59**(3): p. 163-8.

44. Bolliger, C.T., et al., *Use of studded Polyflex stents in patients with neoplastic obstructions of the central airways.* Respiration, 2004. **71**(1): p. 83-7.

45. Freitag, L., et al., *Towards Individualized Tracheobronchial Stents: Technical, Practical and Legal Considerations.* Respiration, 2017. **94**(5): p. 442-456.

46. Freitag, L., et al., *Clinical evaluation of a new bifurcated dynamic airway stent: a 5-year experience with 135 patients.* Thorac Cardiovasc Surg, 1997. **45**(1): p. 6-12.

47. Freitag, L., et al., *Mechanical Properties of Airway Stents*. Journal of Bronchology & Interventional Pulmonology, 1995. **2**(4).

48. Nuutinen, J.P., C. Clerc, and P. Törmälä, *Theoretical and experimental evaluation of the radial force of self-expanding braided bioabsorbable stents.* J Biomater Sci Polym Ed, 2003. **14**(7): p. 677-87.

49. Guibert, N., et al., *Treatment of complex airway stenoses using patient-specific 3D-engineered stents: a proof-of-concept study.* Thorax, 2019. **74**(8): p. 810-813.

50. Guibert, N., et al., *Treatment of Post-transplant Complex Airway Stenosis with a Three-Dimensional, Computer-assisted Customized Airway Stent.* Am J Respir Crit Care Med, 2017. **195**(7): p. e31-e33.

51. TR, G., Y. BP, and M. MS, *Application of 3D Printing for Patient-Specific Silicone Stents: 1-Year Follow-Up on 2 Patients.* Respiration, 2018. **96**(5): p. 488-494.

52. Jung, H.S., et al., *The mechanical characteristics and performance evaluation of a newly developed silicone airway stent (GINA stent).* Scientific Reports, 2021. **11**(1): p. 7958.

Abstract in Korean

국문 초록

배경과 목적: 중심 기도 폐쇄는 기관, 주기관지 혹은 우측 중간기관지가 막히는 것으로 정의되며, 이는 종종 호흡곤란, 질식 및 심지어 사망까지 유발할 수도 있다. 수술적인 접근 방법은 근치적 치료의 기회를 제공할 수 있으나 진행성이거나 전이성 암 또는 의학적 상태가 좋지 않은 환자에서는 시행하기가 어렵다. 이러한 경우 경직성 기관지 내시경을 이용하여 기도 스텐트를 삽입해 볼 수 있다. 스텐트는 중심 기도 폐쇄를 즉각적으로 완화해 줄 수 있지만, 때때로 스텐트 이탈, 스텐트 내 점액 저류 및 스텐트 양 끝단의 육아 조직 형성과 같은 심각한 합병증을 유발할 수 있다. 이런 문제점들을 해결하기 위해 연구자들은 동물 모델 실험을 이용하여 스텐트를 개량하고 있다. 선행 연구를 통해 소수의 기관 협착 동물 모델이 수립되어 있으나, 기관 협착을 유발하는데 상당한 시간 (3~8 주)이 소요되는 단점이 있다. 본 연구를 통해 우리는 돼지를 이용하여 기관 협착 동물 모델을 좀 더 단시간에 확립하려고 시도하였다 (1 부). 그리고 기존 스텐트의 단점을 극복하기 위해 새로운 실리콘 기도 스텐트 (GINA 및 맞춤형 GINA 스텐트)를 개발하였고, 앞서 확립한 기도 협착 동물 모델에서 그 성능을 평가하였다 (2 부 및 3 부). GINA 스텐트는 기관기관지 연골부 접촉면에 직각 삼각형 모양의 외부 링 구조물이 맞물리도록 설계되었고, 막양부 접촉면에는 융기된 3 선 배열을 배치하여 스텐트 이탈 방지를 도모하였다. 또한 기관기관지의 막양부와 유사한 편평한 부분을 통해 실제 기관기관지처럼 스텐트가 역동적으로 수축되게 하여 호기 기류의 속도를 유지함으로써, 기도분비물의 제거가 용이하게 하였으며, 실리콘 재료에 방사선 비투과성 물질을 추가하여 일반 방사선 사진에서 쉽게 위치를 확인할 수 있도록 하였다.

재료 및 방법: 1 부에서 본 연구자들은 돼지에 커프과압삽관 (Cuff-overpressure intubation)과 기관전기소작을 차례로 적용하여 기관 협착이 빠르게 유도되는지 알아보았다. 14 마리의 돼지를 기관전기소작군 (n=3), 커프과압삽관군 및 커프과압삽관-기관전기소작 조합군 (n=8)의 세 개 군으로 나누었다. 내경 9mm 기관내

튜브를 사용하여 커프과압 (200/400/500 mmHg)을 적용하였고, 기관전기소작 (40/60 와트)은 경직성 기관지경을 통해 전기응고기를 사용하여 시행하였다. 중재 후 3 주간 돼지를 관찰하였고 7 일마다 기관지경 검사를 시행하였다. 기관의 단면적이 50% 이상 감소한 경우에 기관 협착이 유도된 것으로 정의하였다. 2 부에서는 새로 개발한 GINA 스텐트의 기계적 특성을 확인하였고, 앞서 수립한 돼지 기관 협착 모델을 이용하여 새로 개발한 GINA 스텐트의 성능을 평가하였다. 모든 테스트는 GINA 스텐트 [외경(OD, mm): 14; 길이(L, mm): 55]와 Dumon 스텐트 (OD: 14, L: 50)를 비교하는 방식으로 수행되었다. 기계적 특성은 디지털 인장력 측정기를 사용하여 이탈 저항력 (anti-migration force), 팽창력 (expansion force) 및 유연성 (flexibility)을 측정하는 방식으로 이루어졌다. 성능시험은 돼지 기관 협착 모델에 두 스텐트를 삽입한 후 [GINA (n = 4) vs. Dumon (n = 3)], 스텐트 관련 합병증이 발생하는지 3 주간 관찰하는 방법으로 수행되었다. 3 부에서는 GINA 스텐트 디자인과 3D 기술을 접목한 맞춤형 기도 스텐트 (custom GINA stent)를 고안하여 이의 성능을 평가하였다. 돼지의 흉부 컴퓨터단층촬영 데이터를 이용하여 맞춤형 GINA 스텐트를 제작하여 기관 협착이 유발된 돼지에 삽입한 후 3 주간 관찰하는 방식으로 2 마리의 돼지에서 시행되었다.

결과: (1 부) 기관 협착 유발에 소요된 시간은 기관전기소작군에서 14 일, 커프과압삽관-기관전기소작 조합군에서 7 일이었다. 커프과압삽관군에서는 협착이 발생하지 않았다. 커프과압삽관-기관전기소작 조합군에서 200mmHg 이상의 커프 압력으로 1 시간 이상 삽관 후 전기소작 (40 와트)을 수행하였을 때, 7 일 이내에 충분한 기관 협착이 발생하였다. 또한 기관 협착 정도는 커프 압력과 기관 삽관 시간에 비례하여 증가하였다. (2 부) 스텐트의 기계적 특성 비교 결과는 다음과 같다. (GINA vs. Dumon): 이탈 저항력 (18.4 N vs. 12.8 N, P = 0.008); 팽창력 (11.9 N vs. 14.5 N, P = 0.008); 유연성 (3.1 N vs. 4.5 N, P = 0.008). 성능시험 결과는 다음과 같다. (GINA vs. Dumon): 점액 저류 0/4 대 0/3, 육아 조직 형성 0/4 대 0/3, 스텐트 이탈 1/4 대 2/3. (3 부) 맞춤형 스텐트 제작은 첫 번째 돼지는 16 일, 두 번째 돼지는 7 일이 소요되었다. 맞춤형 스텐트 삽입 후 3 주간 관찰한 결과, 스텐트는 두 마리 모두에서

삽입 위치에서 이탈되지 않았고, 스텐트 내 점액 저류나 스텐트 양 끝단의 육아 조직 형성도 관찰되지 않았다.

결론: (1 부) 커프과압삽관과 전기소작을 함께 적용함으로써 돼지 기관 협착 모델을 빠르게 (7 일 이내) 수립할 수 있었다. (2 부) GINA 스텐트는 Dumon 스텐트와 비교해 더 나은 기계적 특성과 유사한 단기 성능을 보였다. (3 부) 3D 기술을 활용한 맞춤형 기도 스텐트 (custom GINA stent)를 7 일 이내에 제작하였고, 돼지 기관 협착 모델을 이용한 성능시험을 통해 임상 적용 가능성을 확인하였다.

핵심용어: 실리콘 기도 스텐트, 기관 협착, 돼지 기관 협착 모델, 3D 프린팅, 맞춤형 기도 스텐트